The Journal of Neuroscience, April 15, 1996, 16(8):2592–2604

Muscarinic (m2/m4) Receptors Reduce N- and P-type Ca^{2+} Currents in Rat Neostriatal Cholinergic Interneurons through a Fast, Membrane-Delimited, G-Protein Pathway

Zhen Yan and D. James Surmeier

Department of Anatomy and Neurobiology, College of Medicine, University of Tennessee, Memphis, Tennessee 38163

The signaling pathways mediating the muscarinic modulation of Ca^{2+} currents in neostriatal cholinergic interneurons were studied by combined patch-clamp recording and single-cell reverse transcription-PCR. Cholinergic interneurons were identified by the presence of choline acetyltransferase mRNA. These neurons expressed Q-, N-, L-, P-, and R-type Ca^{2+} currents and the mRNA for the $\alpha 1$ subunits believed to form the channels underlying these currents (classes A, B, C, D, and E). Of the interneurons tested, nearly all expressed M2-class (m2, m4) receptor mRNAs, whereas m1 receptor mRNA was found in only a subset (~30%) of the sample. The muscarinic agonist oxotremorine methiodide produced a dose-dependent reduction of N- and P-type Ba^{2+} currents through Ca^{2+} channels that was antagonized by atropine. *N*-ethylmaleimide eliminated the modulation, as did preincubation with pertussis toxin. The onset and offset of the modulation were rapid and dose-dependent. The modulation was also attenuated by strong depolarizing prepulses and was not observed in cell-attached membrane patches. Taken together, our results suggest that activation of M2-class muscarinic receptors in cholinergic interneurons reduces N- and P-type Ca^{2+} currents through a membrane-delimited pathway using a $G_{i/o}$-class G-protein. This signaling pathway provides a cellular mechanism for hetero- and homosynaptic control of interneuronal activity and acetylcholine release in the striatum.

Key words: neostriatum; patch clamp; calcium current; cholinergic interneuron; neuromodulation; acetylcholine; PCR; muscarinic receptor

Disordered intrastriatal cholinergic signaling is a major factor in the etiology of Parkinson's disease (Barbeau, 1962; Wooten, 1990). This innervation is derived exclusively from giant aspiny interneurons that give rise to striatal concentrations of acetylcholine (ACh), cholinesterase, and choline acetyltransferase (ChAT) that are among the highest in the brain (McGeer et al., 1974; Cheney et al., 1975; Graybiel, 1990). The widely ramifying axonal arbors of these interneurons exert an important neuromodulatory influence on medium spiny neurons projecting to the globus pallidum and substantia nigra (Misgeld et al., 1980, 1986; Akins et al., 1990; Howe and Surmeier, 1995).

Cholinergic interneuronal activity and the release of ACh are also subject to cholinergic modulation (James and Cubeddu, 1987; Lapchack et al., 1989; Dolezal and Wecker, 1990). Ultrastructural studies have shown that cholinergic interneurons make both hetero- and homosynaptic contacts (Phelps et al., 1985; Hersch et al., 1994; Bolam and Bennett, 1995). The postsynaptic effects at these junctions are mediated primarily by G-protein-coupled muscarinic receptors (Lapchak et al., 1989; Vilaró et al., 1992). The five muscarinic receptor genes that have been cloned can be grouped into two classes, an M1-class (m1, m3, m5) and an M2-class (m2, m4), based on their pharmacology and distinctive coupling to signal transduction pathways (Bonner et al., 1987, 1988; Hulme et al., 1990). The identity of the muscarinic receptor subtypes expressed by cholinergic interneurons is controversial. *In situ* hybridization studies have found either extensive colocalization of m1, m2, and m4 mRNAs (Bernard et al., 1992) or principally m2 mRNA, with little or no colocalization of other subtypes (Weiner et al., 1990). Immunocytochemical studies have confirmed the ubiquity of the m2 receptors in presumed interneurons and have suggested that m4 receptors are also expressed by a subset of cells (Hersch et al., 1994).

Both M2- and M1-class receptors are capable of influencing various cellular functions through G-protein-dependent signaling cascades (Hille, 1994; Howe and Surmeier, 1995). For example, voltage-dependent calcium (Ca^{2+}) channels are a common target of modulation by muscarinic receptors of the M2-class. In peripheral autonomic neurons, activation of m4 receptors inhibits N-type Ca^{2+} channels through a membrane-delimited pathway involving a $G_{i/o}$-class protein (Beech et al., 1992; Bernheim et al., 1992; Mathie et al., 1992). A similar pathway seems to be present in medium spiny neostriatal neurons (Howe and Surmeier, 1995) and basal forebrain cholinergic neurons (Allen and Brown, 1993). Because N-type Ca^{2+} channels frequently regulate transmitter release (Dunlap et al., 1995), muscarinic inhibition of these channels provides a possible mechanism for homo- and heterosynaptic regulation of ACh release.

By using a newly developed technique for reverse transcription (RT) and amplification of mRNA in voltage-clamped single cells using PCR (Lambolez et al., 1992; Monyer and Lambolez, 1995), we have attempted to determine whether this signaling model can be applied to neostriatal cholinergic interneurons. Our experi-

Received Oct. 17, 1995; revised Jan. 26, 1996; accepted Jan. 30, 1996.

This work was supported by the National Institute of Neurological Disorders and Stroke Grant NS-28889 to D.J.S. and S. T. Kitai. We also wish to thank Neurex, for their generous gift of SNX-230, and Pfizer, for their gift of ω-agatoxin IVA. We thank Dr. Wen-Jie Song for his help in some of these experiments and Dr. L. Dudkin for her technical help. We also thank Drs. Song, Foehring, and Wilson for critically reading the manuscript.

Correspondence should be addressed to D. J. Surmeier, Department of Anatomy and Neurobiology, University of Tennessee, Memphis, 855 Monroe Avenue, Memphis, TN 38163.

ments argue that most identified cholinergic interneurons express m2 and m4 muscarinic receptors and that acting through a $G_{i/o}$-class G-protein, these receptors produce a rapid, membrane-delimited, voltage-dependent reduction in N- and P-type Ca^{2+} currents. These findings provide a cellular and molecular framework within which hetero- and homosynaptic connections of cholinergic interneurons can be understood.

MATERIALS AND METHODS

Acute-dissociation procedure. Neostriatal neurons from adult (>4 weeks old) rats were dissociated acutely, using procedures similar to those we have described previously (Bargas et al., 1994; Surmeier et al., 1995). In brief, rats were anesthetized with methoxyflurane and then decapitated; brains were quickly removed, iced, and blocked for slicing. The blocked tissue was cut into 400 μm slices with a Vibroslice (Campden Instruments, London, UK) while bathed in a low Ca^{2+} (100 μM), HEPES-buffered salt solution containing (in mM): 140 sodium isethionate, 2 KCl, 4 $MgCl_2$, 0.1 $CaCl_2$, 23 glucose, 15 HEPES, pH 7.4 (300–305 mOsm/l). Slices were then incubated for 1–6 hr at room temperature (20–22°C) in a $NaHCO_3$-buffered saline bubbled with 95% O_2/5% CO_2 containing (in mM): 126 NaCl, 2.5 KCl, 2 $CaCl_2$, 2 $MgCl_2$, 26 $NaHCO_3$ 1.25 NaH_2PO_4,1 pyruvic acid, 0.2 ascorbic acid, 0.1 N^G-nitro-L-arginine, 1 kynurenic acid, 10 glucose, pH 7.4 with NaOH (300–305 mOsm/l). All reagents were obtained from Sigma (St. Louis, MO). Slices were then removed into the low Ca^{2+} buffer, and regions of the dorsal neostriatum were dissected with the aid of a dissecting microscope and placed in an oxygenated Cell-Stir chamber (Wheaton, Millville, NJ) containing pronase (Sigma protease Type XIV, 1–3 mg/ml) in HEPES-buffered HBSS (Sigma) at 35°C. Dissections were limited to tissue rostral to the anterior commissure to reduce the possibility of contamination from the globus pallidus. After 20–40 min of enzyme digestion, tissue was rinsed three times in the low Ca^{2+}, HEPES-buffered saline and dissociated mechanically with a graded series of fire-polished Pasteur pipettes. The cell suspension was then plated into a 35 mm Lux petri dish mounted on the stage of an inverted microscope containing HEPES-buffered HBSS saline.

In some experiments requiring prolonged incubation with reagents (e.g., pertussis toxin), cultured interneurons were used. Cultures were established and maintained as described previously (Surmeier et al., 1988; Bargas et al., 1991).

Whole-cell recordings. Standard techniques were used in whole-cell recordings of Ba^{2+} currents through Ca^{2+} channels (Hamill et al., 1981; Bargas et al., 1994). Electrodes were pulled from Corning 7052 glass and fire-polished before use. The internal solution consisted of (in mM): 180 *N*-methyl-D-glucamine (NMG), 40 HEPES, 4 $MgCl_2$, 0.1 1,2 bis-(o-aminophenoxy)-ethane-N,N,N′,N′-tetraacetic acid (BAPTA), 12 phosphocreatine, 2 Na_2ATP, 0.2 Na_3GTP, 0.1 leupeptin, pH 7.2–3.0 with H_2SO_4 (265–270 mOsm/l). The pH of NMG solutions was measured with a Corning Model 476570 probe. The external solution consisted of (in mM): 135 NaCl, 20 CsCl, 1 $MgCl_2$, 10 HEPES, 0.001 TTX, 2 $BaCl_2$, 10 glucose, pH 7.3 with NaOH (300–305 mOsm/l).

Muscarinic receptor ligands [oxotremorine methiodide (oxo-M), carbachol, atropine (RBI, Natick, MA)] were made up as concentrated stocks in water and stored at 5°C. The cyclic AMP (cAMP) analog 8-(4-chlorophenolthio)-adenosine 3′:5′-cyclic monophosphate (cpt-cAMP) (Sigma) was made up on the day of the experiment. Calcium channel blockers ω-conotoxin (ω-CgTx) GVIA (Peninsula Laboratories, Belmont, CA; RBI; Calbiochem, San Diego, CA), ω-agatoxin (ω-AgTx) IVA (a gift from Pfizer, Groton, CT), ω-conotoxin (ω-CTx) MVIIC (a gift from the Neurex Corporation, Menlo Park, CA) were made up as concentrated stocks in water, aliquoted, and frozen; aliquots were thawed and diluted the day of use. Final dilutions were made in external media containing 0.01–0.1% cytochrome C. Nifedipine and (−)Bay K 8644 (RBI) were made up as concentrated stocks in 95% ethanol and diluted immediately before use. These solutions were protected from ambient light. The involvement of $G_{i/o}$ proteins was studied using *N*-ethylmaleimide (NEM) (Sigma) and pertussis toxin holotoxin (PTX) (Calbiochem). PTX (100 ng/ml) was added to the growth medium of cultured neostriatal neurons 24 hr before recording; sister cultures were used as controls.

Recordings were obtained with an Axon Instruments (Foster City, CA) 200A patch-clamp amplifier and controlled and monitored with a Quadra 900 Macintosh computer running AxoData (version 1.1) with a 125 KHz interface (Instrutech, Greatneck, NY). Electrode resistances were typically 2–4 MΩ in the bath. After seal rupture, series resistance (4–10 MΩ) was compensated (70–90%) and periodically monitored. Recordings were made only from large neurons (>10 pF) that had short (<75 μm) proximal dendrites. The adequacy of voltage control was assessed after compensation by examining the tail currents generated by strong depolarizations. Cells in which tail currents did not decay rapidly and smoothly at subthreshold potentials were discarded. Drugs were applied with a gravity-fed "sewer pipe" manifold system. The application capillary (~150 μm, inner diameter) was positioned a few hundred micrometers from the cell under study. Solution changes were effected by electronic valves controlling the inflow to a manifold feeding a single outlet capillary. Solution changes typically were complete within <1 sec; the time constant of Cd^{2+} block of Ca^{2+} current was 300 msec.

Cell-attached patch recording. Recordings were obtained with an internal solution consisting of (in mM): 110 $BaCl_2$, 10 HEPES, pH 7.4, with TEA hydroxide. Electrodes were made as for whole-cell recordings except that they were coated with Sylgard. After seal formation, the transmembrane potential was nominally zeroed by bathing the cell in an isotonic K^+ solution containing (in mM): 140 potassium gluconate, 1 $MgCl_2$, 5 EGTA, 10 HEPES, 5 glucose, pH 7.4, with KOH (300–305 mOsm/l). Transmembrane currents were evoked by stepping the electrode to −20 mV from a holding potential of +80 mV. The protocol is shown with the conventional polarity in the figures for clarity.

Statistical methods. Data analyses were performed with AxoGraph (Axon Instruments, version 2.0) and Kaleidagraph (version 3.0.4, Albeck Software, Reading, PA). Box plots were used for graphic presentation of the data because of the small sample sizes (Tukey, 1977). The box plot represents the distribution as a box with the median as a central line and the hinges as the edges of the box (the hinges divide the upper and lower distributions in half). The inner fences (shown as a line originating from the edges of the box) run to the limits of the distribution, excluding outliers (defined as points that are >1.5 times the interquartile range beyond the interquartiles; Tukey, 1977); outliers are shown as *asterisks* or *circles*.

Dose–response data were fitted with a Langmuir isotherm curve: $I = I_1(1 + [M]/EC_{50})^{-1} + I_0$, where I_1 and I_0 represented the reducible and nonreducible part of current, respectively; [M] was the agonist concentration; EC_{50} was the half-maximal concentration of agonist. The onset of the muscarinic modulation was fitted with a single or double exponential curve of the form: $I = I_0 + I_1\exp(-(t - t_0)/\tau_1) + I_2\exp(-(t - t_0)/\tau_2)$, where I was peak current, t was time, and t_o was the time at which the drug was applied. Nonparametric statistics were computed with SYSTAT (version 5, SYSTAT, Evanston, IL). Mann–Whitney U tests were performed to compare groups.

Single-neuron RNA harvest and RT-PCR analysis. After recording, cells were lifted up into a stream of control solution and aspirated into the electrode by negative pressure. Electrodes contained ~5 μl of sterile recording solution (see above). The capillary glass used for making electrodes had been autoclaved and heated to 150°C for 2 hr. Sterile gloves were worn during the procedure to minimize RNase contamination.

After aspiration, the electrode was broken, and contents were ejected into a 0.5 ml Eppendorf tube containing 5 μl diethyl pyrocarbonate-treated water, 1 μl RNAsin (28,000 U/ml), 1 μl dithiothreitol (DTT) (0.1 M), and 1 μl of either oligo(dT) (0.5 μg/μl) or random hexanucleotides (50 ng/μl). The mixture was heated to 70°C for 10 min and incubated on ice for 1 min. Single-strand cDNA was synthesized from the cellular mRNA by adding SuperScript II RT (1 μl, 200 U/μl) and buffer (4 μl, 5× First Strand Buffer: 250 mM Tris-HCl, 375 mM KCl, 15 mM $MgCl_2$), DTT (1 μl, 0.1 M), and mixed deoxynucleotide triphosphates (dNTPs) (1 μl, 10 mM). After a 10 min incubation at room temperature, the reaction mixture (20 μl) was transferred to a 42°C water bath and incubated for 50 min. The reaction was terminated by heating the mixture to 70°C for 15 min and then icing. The RNA strand in the RNA–DNA hybrid was removed by adding 1 μl RNase H (2 U/μl) and incubated for 20 min at 37°C. All reagents except RNAsin (Promega, Madison, WI) were obtained from Life Technologies (Grand Island, NY). The cDNA from the RT of RNA in single neostriatal neurons was subjected to PCR to detect the expression of various mRNAs.

The ChAT mRNA (Brice et al., 1989) was identified using a pair of primers flanking a splicing site near the 3′ terminus of the coding region. The upper primer was 5′-ATG GCC ATT GAC AAC CAT CTT CTG (nucleotides 1729–1752) and located on exon 14. The lower primer was 5′-CCT TGA ACT GCA GAG GTC TCT CAT (nucleo-

tides 2029–2052) and located on exon 15. The size of the amplified ChAT cDNA was 324 bp.

The m1–m5 subtype-specific primers were designed against the region coding for the third cytoplasmic loop (i3). Primers used for m1 receptor mRNA (Genbank accession number M16406) detection were 5′-AGC AGC TCA GAG AGG TCA CAG CCA-3′ (nucleotides 857–880) and 5′-GGG CCT CTT GAC TGT ATT TGG GGA-3′ (nucleotides 1106–1129). The size of the amplified m1 cDNA was 273 bp. Primers used for m2 receptor mRNA (Genbank accession number J03025) detection were 5′-CAA GAC CCA GTA TCT CCA AGT CTG-3′ (nucleotides 1133–1156) and 5′-CGA CGA CCC AAC TAG TTC TAC AGT-3′ (nucleotides 1478–1501). The size of the amplified m2 cDNA was 369 bp. Primers used for m3 receptor mRNA (Genbank accession number M16407) detection were 5′-ACA GAA GCG GAG GCA GAA AAC TTT-3′ (nucleotides 854–877) and 5′-CTT GAA GGA CAG AGG TAG AGT AGC-3′ (nucleotides 1391–1414). The size of the amplified m3 cDNA was 561 bp. Primers used for m4 receptor mRNA (Genbank accession number M14609) detection were 5′-AAG GAG AAG AAG GCC AAG ACT CTG-3′ (nucleotides 695–718) and 5′-GCG AGC AAT GCT GGC AAA CTT TCG-3′ (nucleotides 1115–1138). The size of the amplified m4 cDNA was 444 bp. Primers used for m5 receptor mRNA (Genbank accession number M22926) detection were 5′-TGT AGC AGC TAC CCC TCT TCA GAG-3′ (nucleotides 1877–1900) and 5′-AGC AGC AGC TGG AGA CAG AAA GTA-3′ (nucleotides 2051–2074). The size of the amplified m5 cDNA was 198 bp.

cDNAs reverse-transcribed from class A–E mRNAs coding for Ca^{2+} channel $\alpha 1$ subunits were amplified using nested primers targeting the C-terminal regions. The outer pair of primers for rat brain A (rbA) cDNA (Genbank accession number M64373; Starr et al., 1991) were 5′-GCA GAA CCG GAC ACC ACT CAT-3′ (nucleotides 5793–5813) and 5′-GGG ATG ATG GTG ATG ATG GTG G-3′ (nucleotides 6495–6516); the inner pair of primers for rbA were 5′-ATG GGA ACT GAT GGC TAC TCA GAC-3′ (nucleotides 6064–6087) and 5′-TTG GGT GGT CAT GCT CAG ATC TGT-3′ (nucleotides 6391–6414). This set yielded a product of 350 bp.

The outer pair of primers for rbB cDNA (Genbank accession number M92905; Dubel et al., 1992) were 5′-TTC CTG TGA CCG CTT TGG G-3′ (nucleotides 6375–6393) and 5′-TGT ATC CTC AGG CAG GTT GTGG-3′ (nucleotides 6801–6822); the inner pair of primers for rbB were 5′-ATG TCA ACA TCT GGT GCT AGC ACG-3′ (nucleotides 6511–6534) and 5′-GAG CAG GGC ATT GTG TTC AGA AAG-3′ (nucleotides 6685–6708). This set yielded a product of 197 bp.

The outer pair of primers for rbC cDNA (Genbank accession number M67516; Snutch et al., 1991) were 5′-CGA TGA AAA CCG ACA ACT GAC C-3′ (nucleotides 5858–5879) and 5′-GAA ATC AAG ACC GCT TCC ACC-3′ (nucleotides 6380–6400); the inner pair of primers for rbC were 5′-CAA AAG GAT CAA GGG GGA GAC A-3′ (nucleotides 5988–6011) and 5′-GCT GCT GTT GAG TTT CTC ACT GGA-3′ (nucleotides 6204–6227). This set yielded a product of 239 bp.

The outer pair of primers for rbD cDNA (Genbank accession number M57682; Hui et al., 1991) were 5′-GAC TCA GAT TAC AAC CCA GGA GAG-3′ (nucleotides 4793–4816) and 5′-TTC AAG CAT CTG TAG GGC GAT CGT-3′ (nucleotides 5432–5455); the inner pair of primers for rbD were 5′-TGT GGG AGC AAC TTT GCC ATT GTC-3′ (nucleotides 4826–4849) and 5′-GGT GTT CTT CGC AGG GTA TTT CCC-3′ (nucleotides 5408–5431). This set yielded a product of 605 bp.

The outer pair of primers for rbE cDNA (Genbank accession number L15453; Soong et al., 1994) were 5′-CAC CAG CAC CCC AAG ACG AAG-3′ (nucleotides 6365–6385) and 5′-CCA GCC TCC GCC GCC GAT AGT-3′ (nucleotides 6766–6786); the inner pair of primers for rbE were 5′-TCC TGA TGG AAG TGA GGG TGG AT-3′ (nucleotides 6476–6499) and 5′-AAG CTA GTA GCT ACA GCT GCC TC-3′ (nucleotides 6678–6700). This set yielded a product of 224 bp.

PCR amplification was carried out with a thermal cycler (MJ Research, Watertown, MA) with thin-walled plastic tubes. Amplification was performed in one of two ways. In the initial experiments, conventional PCR amplification was used for detection of ChAT, muscarinic receptor mRNAs, and Ca^{2+} channel $\alpha 1$-subunit mRNAs. Reaction mixtures contained 2.0–2.5 mM $MgCl_2$, 0.5 mM of each of the dNTPs, 0.8–1.0 μM primers, 2.5 U *Taq*DNA polymerase (Promega), 5 μl 10X Buffer (Promega), and 1–2 μl cDNA template made from the single-cell RT reaction (see above). The thermal cycling program for these PCR amplifications was 94°C for 1 min, 58°C for 1 min, and 74°C for 1.5 min. This was performed for 45 cycles to obtain the signals for ChAT and m1–m5 mRNAs. For the detection of rbA–rbE mRNAs, a first-round (40-cycle) amplification was

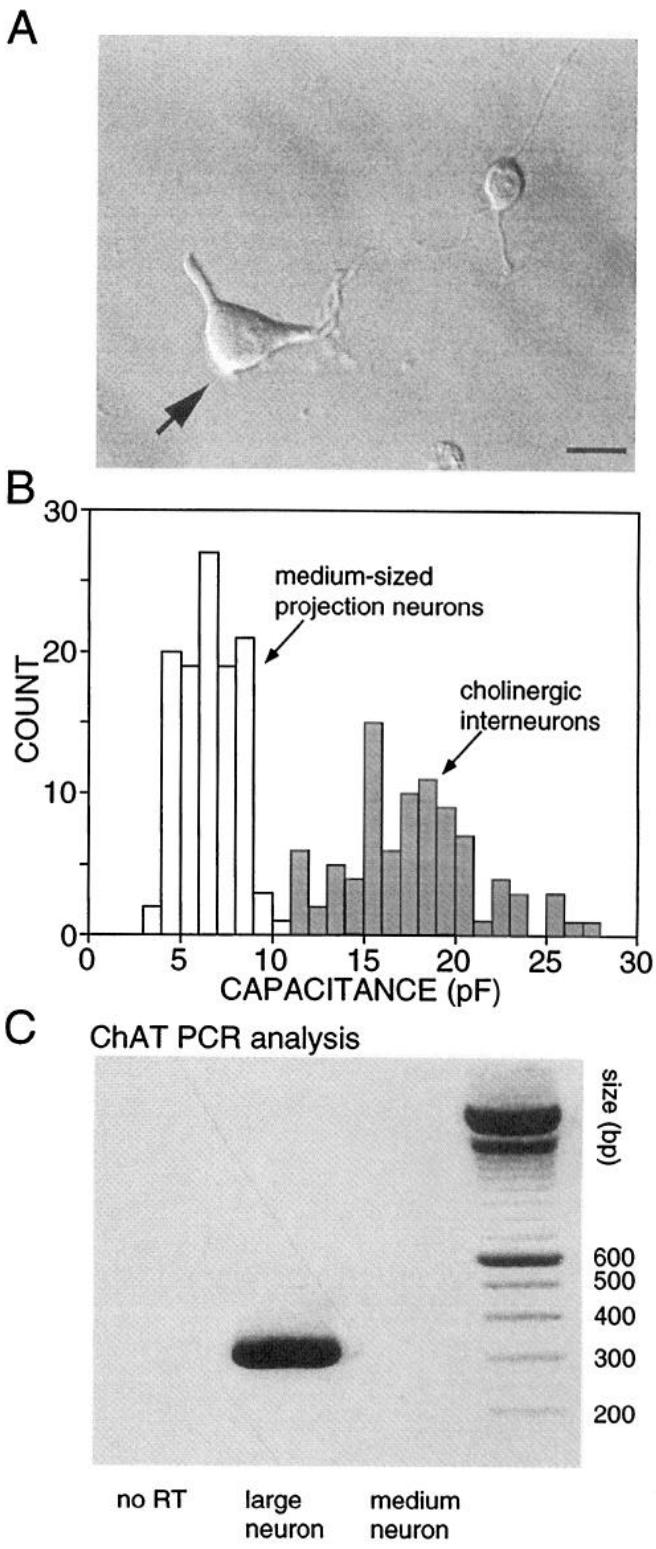

Figure 1. Neostriatal cholinergic interneurons were identified by their large size and expression of ChAT mRNA. *A*, Photomicrograph of acutely isolated neostriatal neurons. *Arrow* points to a large neuron; to the *right* is a medium-sized neuron. Scale bar, 15 μm. *B*, Histogram of whole-cell capacitance estimates from a sample of medium- and large-sized neurons. Neurons with capacitances in the *shaded area* were consistently positive for ChAT mRNA ($n = 71$). *C*, Photomicrograph of PCR products separated on an ethidium bromide-stained 2% agarose gel. *Left lane* ("no RT") was loaded with the products derived from a large neuron in which the reverse transcriptase was omitted. *Middle lane* ("large neuron") was loaded with the product derived from a single large neuron; *right lane* was loaded with the product derived from a medium-sized neuron.

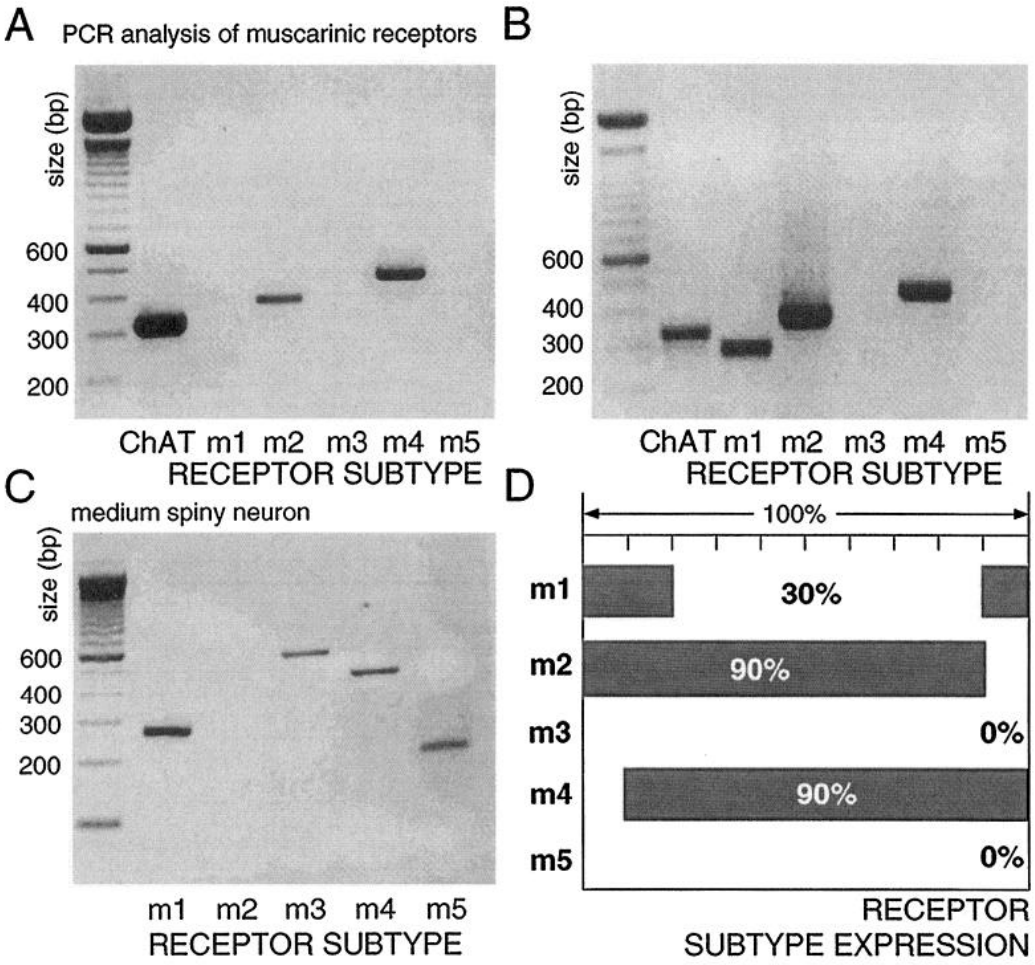

Figure 2. ChAT interneurons expressed primarily M2-class receptor mRNAs. *A*, PCR profile of a single ChAT-positive neuron having detectable levels of m2 and m4 mRNAs. *B*, A PCR profile of a ChAT-positive neuron having m1, m2, and m4 mRNAs. *C*, A PCR profile of a retrogradely labeled striatonigral neuron showing detectable levels of m1, m3, m4, and m5 mRNA. *D*, Bar plot showing the coordinated expression of muscarinic receptor subtypes m1–m5 in ChAT-positive neurons detected by the multiplex PCR method ($n = 10$).

performed using the outer pairs of primers, and then a 2 μl PCR product was taken as template for the second-round (40-cycle) amplification using the inner pairs of primers.

It is possible using this procedure to miss very low abundance templates. For example, if a cell had 10 copies of a particular mRNA and we assume complete RT into cDNA, there is a substantial probability of obtaining no signal when using one tenth or one fifth of the total complement of cDNA. This was a major concern in the analysis of muscarinic receptor mRNAs. To minimize this problem, a two-stage multiplex amplification was performed. In the first step, the muscarinic receptor cDNAs were amplified selectively using half of the single-cell cDNA (10 μl) as a template in a multiplex PCR reaction. All five muscarinic receptor primers were added to a reaction mixture containing the same reagents as with conventional PCR, except for slightly elevated

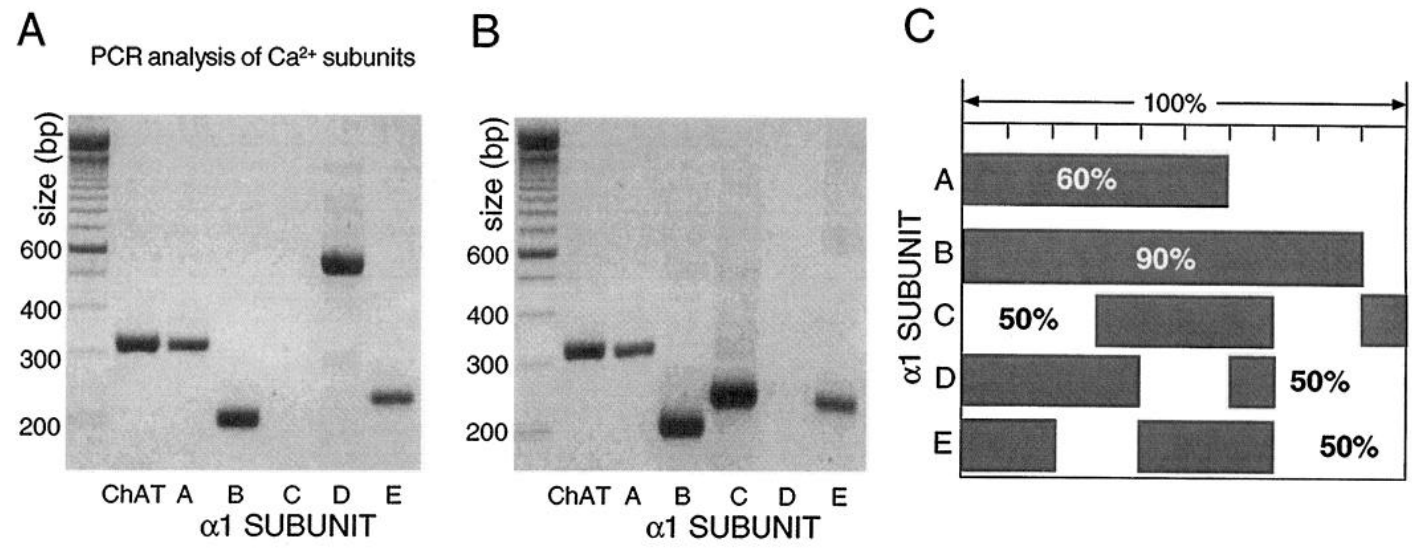

Figure 3. ChAT interneurons expressed mRNA for Ca^{2+} channel α1 subunits. *A*, PCR profile of a single ChAT-positive neuron showing expression of A, B, D, and E mRNA. *B*, PCR profile of a ChAT-positive neuron showing expression of A, B, C, and E mRNA. *C*, Bar plot showing the coordinated expression of class A, B, C, D, and E mRNAs in ChAT-positive neurons ($n = 10$).

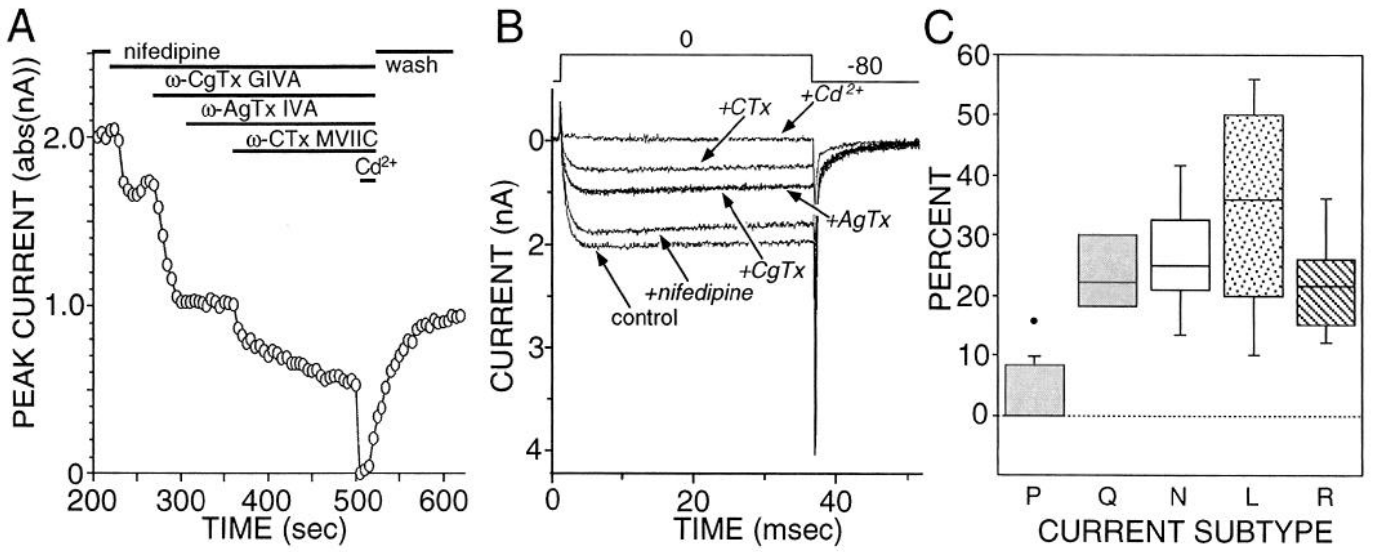

Figure 4. ChAT interneurons exhibited several types of HVA-type currents. *A*, Plot of peak current evoked by a voltage step to 0 mV as a function of time and antagonist application. Duration of antagonist application is denoted by a *bar*. *B*, Current traces from the records used to construct *A* at various time points after application of channel antagonists. *C*, Box plot summary of the percentage block by each antagonist in a large sample of interneurons. *P* ($n = 11$), *Q* ($n = 4$), *N* ($n = 9$), *L* ($n = 17$), and *R* ($n = 4$) current types are shown. The percentage of Q-type current may be underestimated because steady-state block was not always achieved.

$MgCl_2$ (4.0 mM) and dNTPs (1.0 mM). Twenty cycles were performed using the parameters given above. An aliquot of this PCR product (2 μl) was then used as a template for a second-round of conventional PCR amplification (40-cycle) with each pair of subtype-specific primers.

Products were visualized by staining with ethidium bromide and analyzed by electrophoresis in 2% agarose gels. All products were sequenced using a dye-termination procedure by either the University of Tennessee Molecular Resource Center or the St. Jude Children's Research Hospital (Memphis, TN) sequencing facility and were found to match the published sequences.

Care was taken to ensure that the PCR signal arose from cellular mRNA. In addition to the controls noted above (e.g., primers that span splice sites), negative controls for contamination from extraneous and genomic DNA were run for every batch of neurons. To ensure that genomic DNA did not contribute to the PCR products, neurons were aspirated and processed in the normal manner, except that the reverse transcriptase was omitted. Contamination from extraneous sources was checked by replacing the cellular template with water. Both controls were consistently negative in these experiments.

RESULTS

Large neurons express ChAT mRNA

Although giant aspiny, cholinergic interneurons comprise only 1–3% of the total neuronal population in the dorsal striatum, large neurons were visualized readily in the acutely dissociated preparation. As shown in Figure 1*A*, large neurons with truncated dendrites were clearly distinguishable from the smaller, medium-sized neurons that constituted the vast majority of dissociated cells. The distribution of whole-cell capacitance measurements from a large sample of neurons was distinctly bimodal (Fig. 1*B*). Neurons with whole-cell capacitances >10 pF that were subjected to RT-PCR analysis for ChAT mRNA consistently yielded product of the expected size and sequence (Fig. 1*C*). Medium-sized neurons, on the other hand, were consistently negative for ChAT mRNA, as expected of this largely GABAergic population. Large neostriatal neurons expressing ChAT mRNA were assumed to be cholinergic interneurons.

Cholinergic neurons express primarily M2-class (m2, m4) receptor mRNA

To determine how the expression of muscarinic receptor subtypes was coordinated, 20 single neurons were analyzed using RT-PCR techniques. Two PCR strategies were used. Ten cells were studied using conventional PCR with one tenth of the cellular cDNA as a template. Another 10 cells were studied using a multiplex protocol in which half of the cellular cDNA was used as a template. If an mRNA was of relatively high abundance, its detection frequency should be the same with both protocols. If an mRNA was of relatively low abundance, however, using only one tenth of the cDNA should lower the frequency of detection. Lastly, if an mRNA was present and abundant in a distinct subset of neurons, then the detection frequency should be <100% and unaltered by reducing template concentration.

Both protocols revealed that nearly all (9 of 10, both protocols) ChAT neurons had detectable levels of m2 mRNA, indicating that m2 mRNA is expressed abundantly in essentially all cells. Using multiplex PCR, nearly all (9 of 10) ChAT neurons had detectable levels of m4 mRNA, whereas only a small subset (3 of 10) of ChAT neurons had detectable levels when one tenth of the cellular cDNA was used, suggesting that m4 mRNA is expressed in nearly all ChAT neurons but in low abundance (Fig. 2*A*). Both methods detected m1 mRNA in only 20–30% of ChAT neurons (3 of 10 using half of the aliquot; 2 of 10 using one tenth of the aliquot), which suggests that it was present in a distinct subset of interneurons (Fig. 2*B*). As a control for the efficiency of m1, m3, and m5 primer pairs to amplify single-cell templates, medium spiny neurons were also analyzed. In Figure 2*C*, a profile of a medium spiny neuron expressing these mRNAs is shown. A *bar plot* depicting the coordinated expression of muscarinic receptor mRNAs in the 10 cells subjected to multiplex PCR analysis is shown in Figure 2*D*.

Cholinergic neurons express a heterogeneous population of Ca^{2+} channels

Before examining the neuromodulatory impact of muscarinic receptors on Ca^{2+} currents, a preliminary analysis of the molecular and pharmacological properties of the channels underlying these currents was performed. First, profiles for class A–E α1-subunit mRNA were constructed for individual neurons, using a nested PCR analysis. The α1 subunit forms the channel

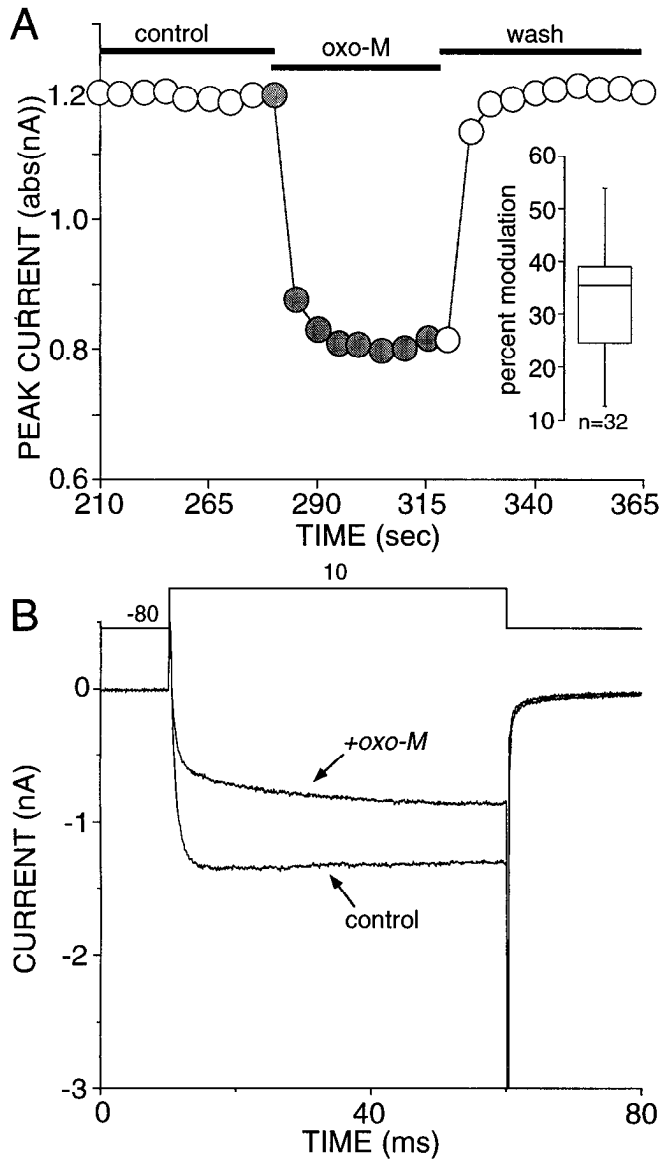

Figure 5. Muscarinic agonists produced a rapid decrease in Ba^{2+} currents. *A*, Plot of peak current evoked by a voltage step to +10 mV as a function of time and agonist application. Oxo-M rapidly and reversibly reduced peak currents. *Inset* is a box plot showing the reduction in peak current in a sample of 32 large neurons. *B*, Current traces from the data used to construct *A* before and during oxo-M application.

pore and is a principal determinant of channel pharmacology (Tsien et al., 1991; Snutch and Reiner, 1992). A typical single-cell profile is shown in Figure 3*A*. This neuron expressed detectable levels of class A, B, D, and E mRNA. A profile from another neuron is shown in Figure 3*B*. The expression pattern was similar except that class C mRNA was detected and class D was not. These two mRNAs, both of which code for an L-type subunit, were rarely detected in the same neuron. Class B and either class C or D products were consistently the most abundant and commonly detected in these experiments. A diagram depicting the coordinated expression of the α1-subunit mRNAs for a sample of 10 interneurons is shown in Figure 3*C*. Class B mRNA was detected in 90% of the neurons, suggesting that it was of high abundance. The lower detection percentages for

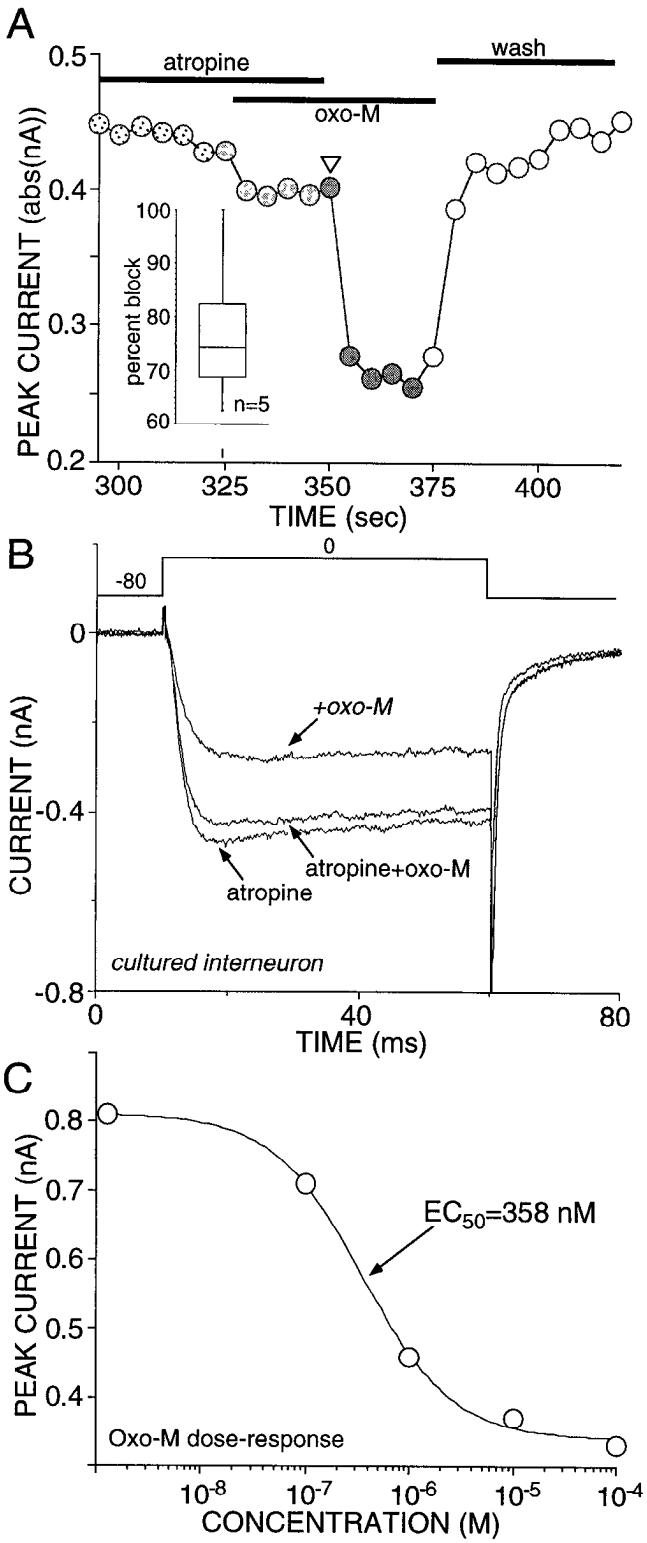

Figure 6. The modulation by oxo-M was antagonized by atropine and dose-dependent. *A*, Plot of peak current evoked in a large cultured interneuron by a step to 0 mV as a function of time and ligand application. The application of oxo-M (1 μM) in the presence of atropine (1 μM) had only a modest effect; washing off the antagonist led to a substantial reduction in currents. *B*, Representative current traces from the data used to construct *A*. *C*, Dose–response curve from an acutely isolated large neuron. Peak current evoked by a step to 0 mV is plotted as a function of agonist concentration. The *solid line* is a least squares fit of a Langmuir isotherm with an EC_{50} of 358 nM.

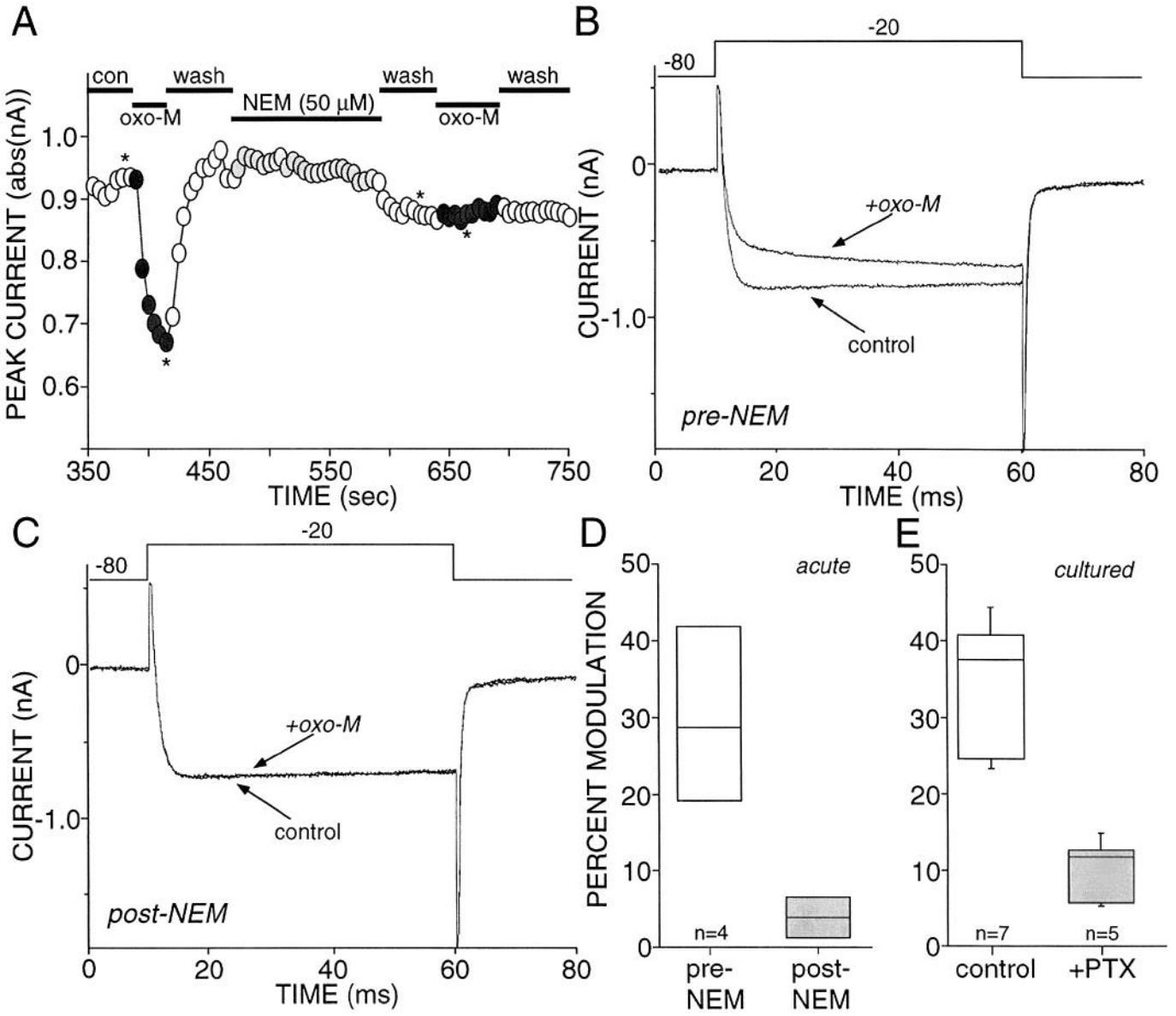

Figure 7. The modulation by oxo-M used a $G_{i/o}$-class G-protein. *A*, Plot of peak current evoked in a dissociated large interneuron by a step to −20mV as a function of time and drug application. Oxo-M (10 μM) reduced peak currents; the reduction was eliminated by 2 min application of NEM (50 μM). *B*, Representative current traces showing the modulation effect of oxo-M before application of NEM. *C*, Representative current traces showing the blocked effect of oxo-M after application of NEM. *D*, Box plot of the percentage reduction in peak current produced by oxo-M (10 μM) in dissociated large neurons pre- and post-NEM (50 μM). *E*, Box plot of the percentage reduction in peak current produced by oxo-M (10 μM) in large cultured neurons with and without PTX (100 ng/ml) exposure for 24 hr.

mRNA in the other classes may have been a reflection of lower abundance rather than their absence, because currents believed to be carried by these subunits were always present (see below; also note that the multiplex analysis was not performed for Ca^{2+} channel subunits).

Next, a pharmacological analysis of the Ba^{2+} currents carried by these channels was performed. These studies yielded a picture consistent with the molecular analysis. Data from one cholinergic interneuron are shown in Figure 4*A*. In this figure, the peak current evoked by a voltage step to 0 mV is plotted as a function of time during the application of specific channel antagonists. Representative current traces from this experiment are shown in Figure 4*B*. As shown in the plot, the application of the L-type channel antagonist nifedipine (5 μM) blocked a component of the current in this cell in agreement with the presence of class C or D mRNA in nearly every interneuron. ω-CgTx GVIA (1 μM), a specific antagonist of N-type channels, also blocked a substantial portion of the whole-cell current, as predicted from the presence of class B mRNA. In contrast, ω-AgTx IVA (50 nM) did not affect currents in this neuron, indicating that P-type currents were not present in the soma or proximal dendrites. The other channel subtype thought to be formed from class A α1 subunits, the Q-type channel, is blocked by ω-CTx MVIIC in the presence of low nanomolar concentrations of ω-AgTx IVA and micromolar ω-CgTx GVIA (Stea et al., 1994; Randall and Tsien, 1995). In this cell, ω-CTx MVIIC (2 μM) significantly reduced whole-cell currents after application of ω-AgTx IVA and ω-CgTx GVIA,

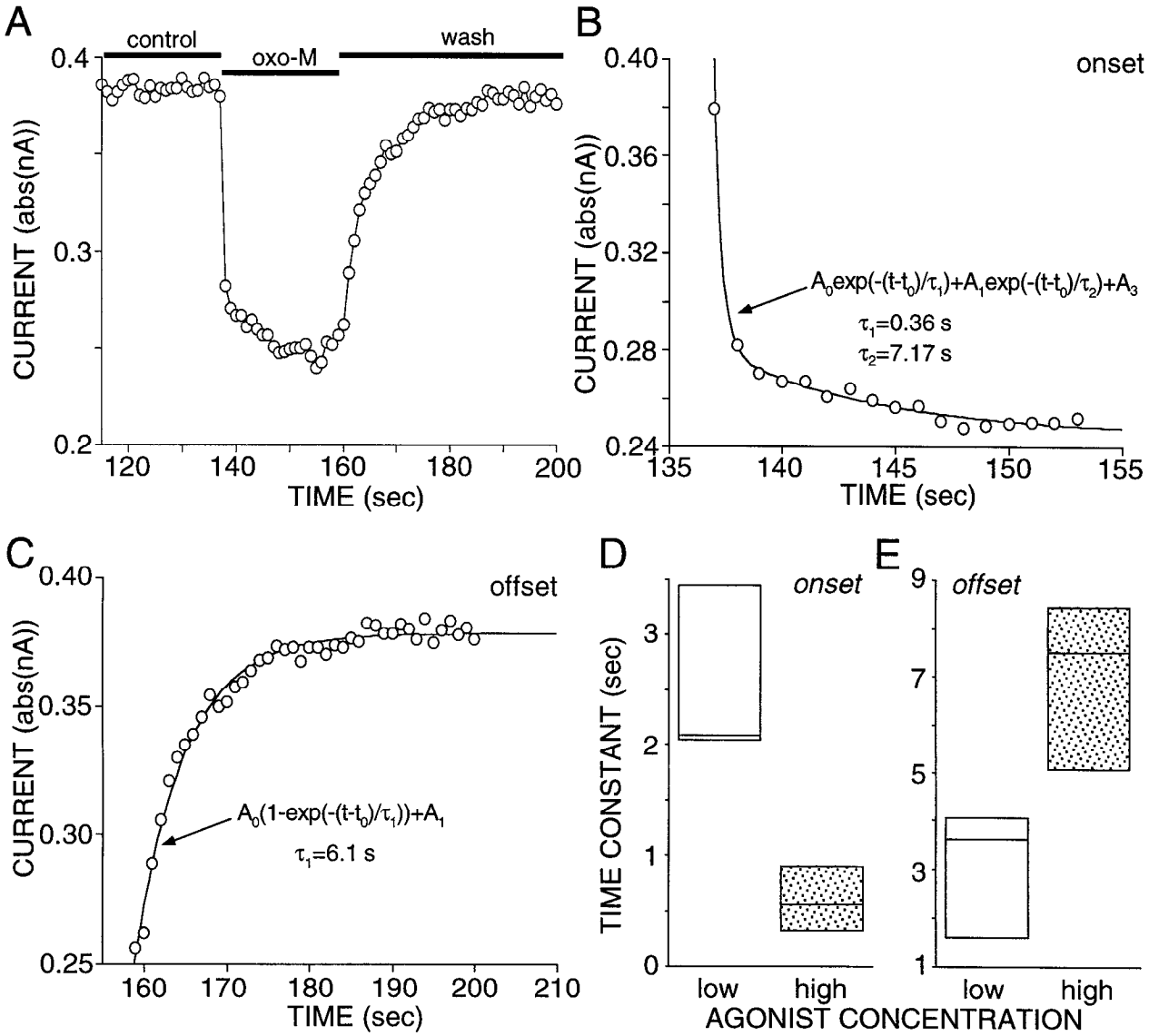

Figure 8. The onset and offset kinetics of the muscarinic modulation were rapid and dose-dependent. *A*, Plot of peak current evoked by a step to 0 mV repeated at 1 Hz as a function of time and oxo-M (500 μM) application. *B*, Biexponential fit of the onset of the modulation. Fitted line was determined by a least squares algorithm; the equation and fitted time constants are shown. *C*, Offset was well fit with a single exponential having a time constant of 6.1 sec. *D*, Box plot summary of onset (fast component) and offset time constants as a function of high (500 μM; $n = 4$) and low (10 μM; $n = 3$) oxo-M concentration.

demonstrating the presence of Q-type channels. A substantial portion of the whole-cell current was unblocked by the combination of L-, N-, P-, and Q-type channel antagonists. This current is often referred to as "resistant" or R-type current and has been hypothesized to be attributable to a channel formed with a class E subunit (Tsien et al., 1995). A statistical summary of experiments testing these antagonists is shown in Figure 4*C*. It must be emphasized that because the dendritic tree was preserved only partially in these neurons, the pharmacological data can be taken as only a rough indication of the proportion of somatodendritic channels of each type. Nevertheless, it is worth noting that N- and L-type currents constituted the largest fraction of the currents recorded from the dissociated neurons, and the mRNAs coding for these channel types (B, C/D) were the most abundant and consistently detected in the RT-PCR experiments.

Muscarinic receptors reduce Ba^{2+} currents through a PTX-sensitive G-protein

The application of the muscarinic agonist oxo-M (10 μM) rapidly and reversibly decreased Ba^{2+} currents through Ca^{2+} channels. In Figure 5*A*, a plot of peak current evoked by slowly repeated voltage steps to +10 mV before, during, and after oxo-M application is shown. The median reduction in peak current by oxo-M at this concentration was just over 35% (see *inset box plot* in *A*). Representative current traces from this experiment are shown in Figure 5*B*. In this cell, as in most neurons, the reduction in peak current was accompanied by a slowing of current activation kinetics (Bean, 1989).

To verify muscarinic receptor mediation, the ability of atropine to antagonize the effect of oxo-M was examined. Atropine (0.1–10 μM) in and of itself decreased Ba^{2+} currents when applied to

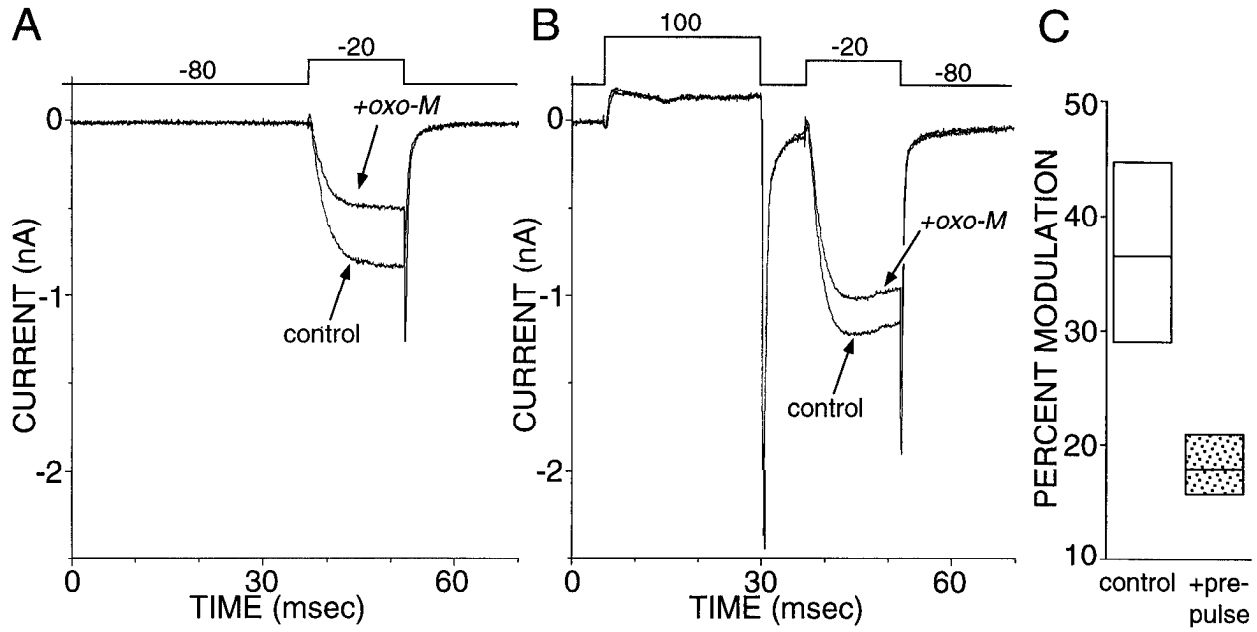

Figure 9. The modulation by muscarinic agonists was attenuated by depolarizing prepulses. *A*, Currents evoked by a step to −20 mV before and after oxo-M (10 μM) application. *B*, Currents in the same neuron evoked by a brief step to +100 mV, a return to −80 mV, and then a test step to −20 mV in the presence and absence of oxo-M. Note that the percentage modulation is reduced after the prepulse. *C*, Box plot summary of the percentage reduction in peak currents produced by oxo-M with and without a depolarizing prepulse (n = 4).

enzyme-treated, dissociated neurons. Cultured interneurons, on the other hand, were not strongly affected by atropine alone. In these neurons, atropine (1 μM) consistently antagonized the modulation by oxo-M (1 μM). Shown in Figure 6*A* is a time course from one of these experiments showing atropine antagonism of the oxo-M modulation. Representative current traces from this experiment are shown in Figure 6*B*. As a further test, dose–response experiments were performed with dissociated interneurons. The modulation by oxo-M was dose-dependent. In the neuron depicted in Figure 6*C*, the EC_{50} was 358 nM; similar values were obtained in two other neurons.

As shown above, the RT-PCR experiments revealed that M2-class (m2, m4) receptor mRNAs were expressed by most interneurons, whereas other muscarinic receptor mRNAs were less common, suggesting that the effects of oxo-M were mediated by M2-class receptors. These receptors couple to intracellular signaling elements through PTX-sensitive G-proteins of the $G_{i/o}$ class (Hulme et al., 1990; Bonner, 1992). If the effects of oxo-M were mediated by a $G_{i/o}$-class G-protein, then NEM (Shapiro et al., 1994) or PTX should block the modulation. Shown in Figure 7*A* is a plot of peak current evoked by a step to −20 mV as a function of time. The modulation produced by oxo-M was eliminated completely by a 2 min application of NEM (50 μM). Figure 7*B,C* shows the oxo-M modulation before and after NEM application, respectively. Similar results were obtained in three other neurons (Fig. 7*D*). Preincubation of cultured interneurons with PTX (100 ng/ml) also significantly reduced the neuromodulatory impact of oxo-M (Fig. 7*E*), confirming the conclusion that the effects of muscarinic agonists were mediated by $G_{i/o}$-class G-proteins.

The muscarinic modulation is rapid

In peripheral autonomic neurons, m4 muscarinic receptors rapidly reduce Ca^{2+} currents through a membrane-delimited, voltage-dependent pathway (Hille, 1994). Because m4 and m2 receptors are linked through the same $G_{i/o}$-class proteins (Hulme et al., 1990; Bonner, 1992), it was our working hypothesis that the phenomenology of the muscarinic signaling in neostriatal cholinergic neurons would be the same as in peripheral autonomic neurons. As a first test of this hypothesis, the onset and offset kinetics of the muscarinic modulation were measured. In peripheral autonomic neurons, the onset kinetics of the muscarinic modulation has a time constant of <1 sec at high agonist concentrations (Bernheim et al., 1991). As shown in Figure 8*A*, the same was true of the modulation in cholinergic interneurons. In this figure, peak currents evoked by a short (30 msec) step to 0 mV are plotted as a function of time. The test pulse was repeated at a rate of 1/sec. When a high concentration (500 μM) of oxo-M was applied, currents were reduced rapidly. The onset of the modulation was typically biexponential, with a fast time constant of <1 sec and a slow time constant of 5–10 sec (Fig. 8*B*). The offset of the modulation was typically monoexponential, with a time constant between 5 and 9 sec (Fig. 8*C*). At lower agonist concentrations (10 μM), the onset kinetics was slower and the offset kinetics faster. A box plot summary of the fast-onset time constants and the offset time constants at high (500 μM) and low (10 μM) concentration of oxo-M is shown in Figure 8*D,E*.

The muscarinic modulation is voltage-dependent

Another characteristic of the muscarinic modulation of Ca^{2+} currents in autonomic neurons (and medium spiny neurons) is that the modulation is attenuated by strong membrane depolarization. This was also a characteristic of the muscarinic modulation in interneurons. As shown above, the currents evoked by a weak depolarizing step from a holding potential of −80 mV were reduced substantially by the application of oxo-M (Fig. 9*A*). When this test stimulus was preceded by a short voltage step to +100 mV, the percentage reduction in the evoked current brought about by oxo-M was reduced significantly (Fig. 9*B*). In a sample of four cells, the median reduction in the absence of a depolarizing

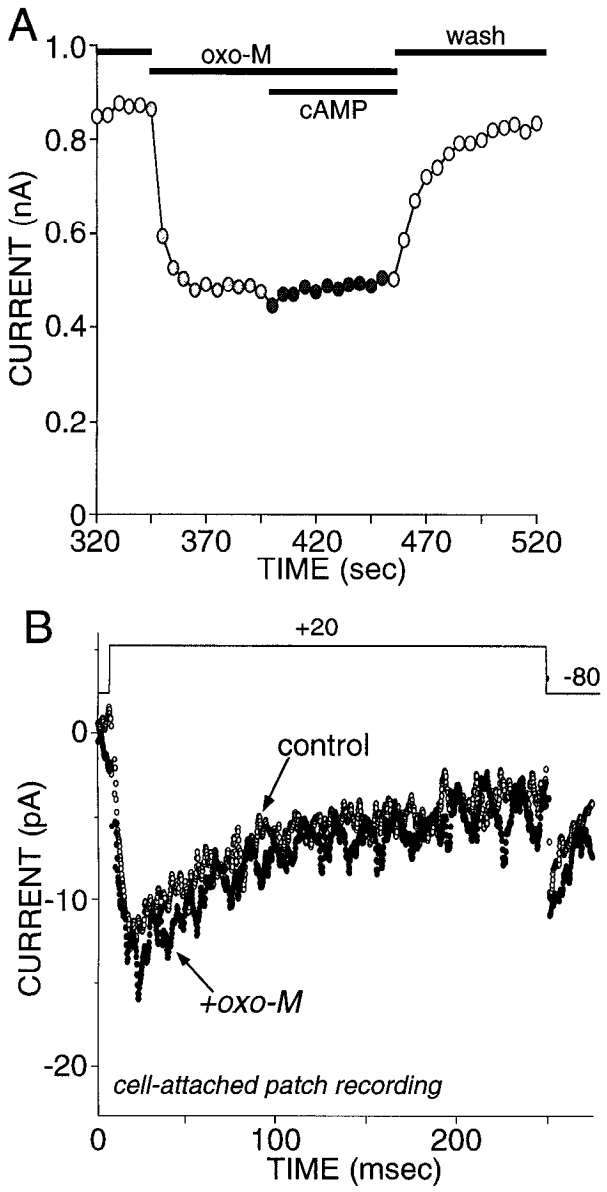

Figure 10. Muscarinic agonists act through a membrane-delimited pathway. *A*, Plot of peak current evoked by a step to 0 mV as a function of time and drug application. Oxo-M (10 μM) reduced peak currents; the reduction was unaffected by the coapplication of cpt-cAMP (500 μM). *B*, Averaged currents (five successive sweeps) evoked in cell-attached patch recordings by a depolarizing voltage step to +20 mV before and during drug application. The application of oxo-M (10 μM) to the bath (via the perfusion pipette) for 2 min had no effect on peak currents. More than 95% of all neurons recorded in the whole-cell configuration responded to oxo-M ($n > 60$). Current polarity has been reversed for clarity.

prepulse was >35%, whereas after a prepulse, the median modulation was ~18% (Fig. 9*C*).

The muscarinic modulation does not employ a cytosolic messenger

M2-class receptors are capable of influencing Ca^{2+} currents through cytosolic second messengers. In the cardiac cells, for example, activation of m2 receptors reduces Ca^{2+} currents by inhibiting adenylyl cyclase, thus reducing cytosolic cAMP levels and protein kinase A activity (Hescheler et al., 1986; Hulme et al., 1990). If this were the mechanism by which muscarinic effects in cholinergic interneurons were mediated, then bath application of the membrane-permeant cAMP analog, cpt-cAMP, should reverse the modulation by countering the reduction in cytosolic cAMP levels. Bath application of cpt-cAMP (500 μM), however, had no effect on the muscarinic modulation of Ba^{2+} currents in any of the neurons tested ($n = 3$) (Fig. 10*A*).

M2-class receptors are also known to reduce Ca^{2+} currents through membrane-delimited pathways that do not depend on cytosolic signals, such as cAMP (Hille, 1994). To test whether M2-class receptors in cholinergic interneurons used such a pathway, cell-attached patch recordings of Ba^{2+} currents were obtained, and oxo-M was applied to the bath (outside the patch). If the signaling pathway were limited to the plane of the membrane, then currents should not be modulated in this recording configuration. In accord with this hypothesis, the currents evoked by depolarization in the cell-attached patches were not modulated by application of oxo-M to the membrane outside the patch ($n = 5$), which suggests that M2-class receptors inhibited currents through a membrane-delimited pathway (Fig. 10*B*).

Muscarinic receptors target N- and P-type currents

In some cell types, such as cardiac myocytes, m2 receptors are capable of reducing current through L-type channels (Hescheler et al., 1986). As shown above, neostriatal cholinergic interneurons express two L-type channels: those with class C (cardiac) α1 subunits and those with class D subunits. To determine whether a cardiac-like pathway was functioning, L-type currents were enhanced by bath application of the dihydropyridine agonist BayK 8644, and oxo-M was applied. As shown in Figure 11*A*, BayK 8644 increased peak ramp currents and slowed deactivation tail currents (Fig. 11*B*). Although oxo-M reduced peak ramp currents, it did not significantly reduce the L-current-dominated, slow, BayK 8644-enhanced tail current. The *inset* in Figure 10*B* is a box plot summary of tail current measurements taken from experiments such as those depicted ($n = 5$). In accordance with these results, application of the L-channel antagonist nifedipine (5 μM) did not reduce the magnitude of the muscarinic modulation ($n = 5$, Fig. 11*C*). These results argue that L-type currents were not affected by muscarinic agonists.

In many neurons, activation of M2-class receptors leads to an inhibition of N- and P-type currents (Hille, 1994; Howe and Surmeier, 1995). To test whether N-type channels were targeted by M2-class receptors in cholinergic interneurons, the ability of the specific N-type antagonist ω-CgTx GVIA to occlude the effects of oxo-M was examined. ω-CgTx GVIA (2 μM) significantly reduced the effects of oxo-M but did not eliminate them. As shown in the plot in Figure 11*C*, the additional block of P-type currents with ω-AgTx IVA (50 nM) was often required to completely occlude the modulation by oxo-M. As shown in the *box plots* summarizing experiments with L-, N-, and P-type channel antagonists, the combination of N- and P-type channel block potently occluded the muscarinic modulation in all neurons ($n = 4$), whereas L-type channel block was without effect ($n = 5$).

DISCUSSION

The interpretation of our results depends, first and foremost, on the assumption that cholinergic interneurons were identified correctly. Two criteria were used: size and the presence of ChAT mRNA. Cholinergic interneurons are often referred to as "giant" aspiny neurons because they are the largest neurons found in the striatum (Phelps et al., 1985; Bolam and Bennett, 1995). Although compelling, size alone is not a sufficient criterion. The presence of

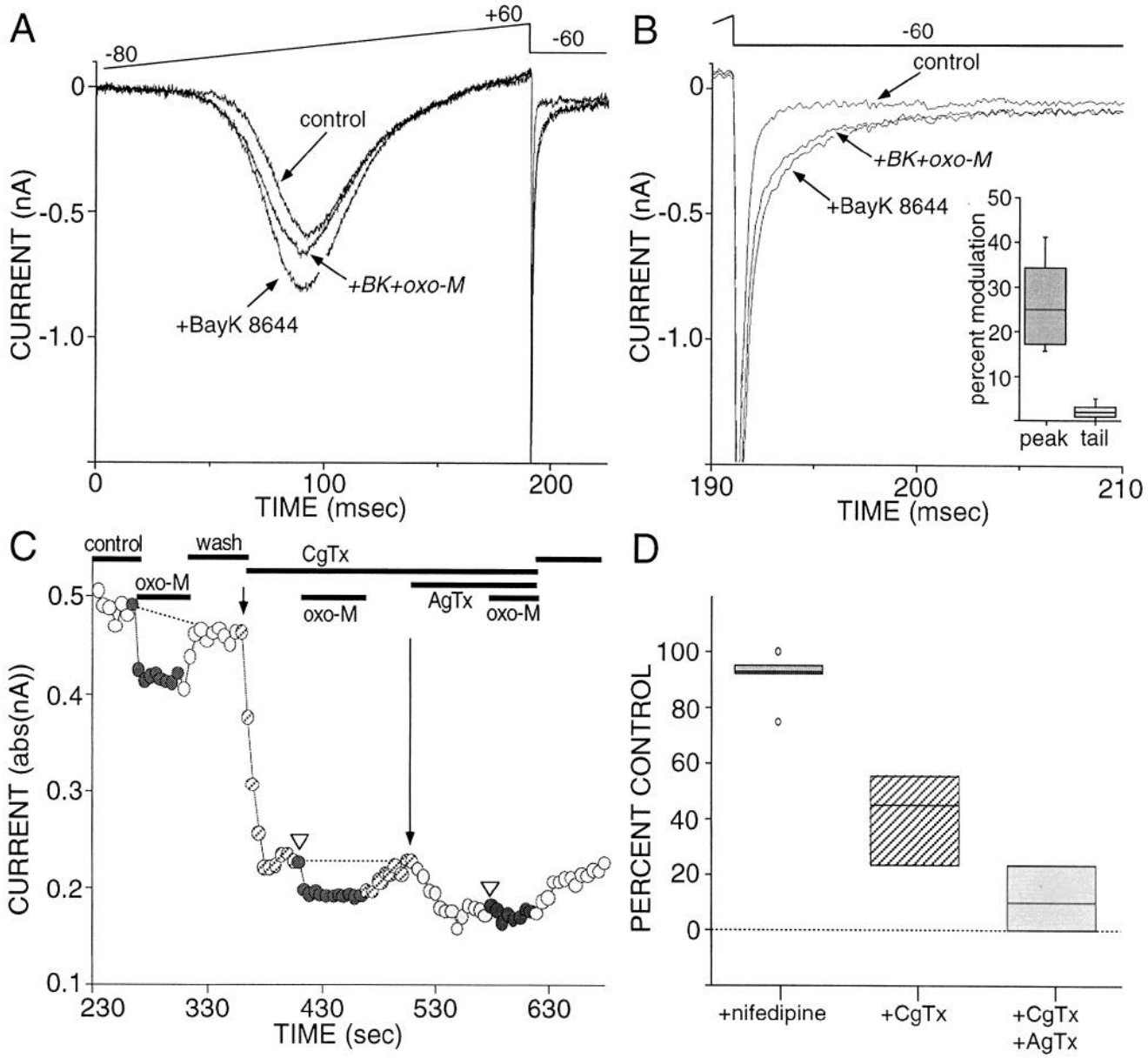

Figure 11. Muscarinic agonists reduced N- and P-type currents but not L-type currents. *A*, Currents evoked by a voltage ramp from −80 to +60 mV. Currents before (control) and during the application of the L-channel agonist (−) Bay K 8644 (1 μM); coapplication of oxo-M (10 μM) reduced peak ramp currents but did not alter slow components of the tail currents. *B*, Expanded view of the tail currents in *A*. Oxo-M had little effect on the slow component of the tail current. *Inset* is a box plot summary of the reduction in peak current and tail current (measured 8 msec into the tail) produced by oxo-M in the presence of Bay K 8644 ($n = 5$). *C*, Plot of peak current evoked by a step to 0 mV as a function of time and drug application. The modulation by oxo-M was reduced by block of N-type channels with ω-CgTx GVIA (2 μM) but was not eliminated. Subsequent block of P-type currents with ω-AgTx IVA (50 nM) completely eliminated the modulation. *D*, Box plot summary of the impact of L-channel [nifedipine (5 μM); $n = 5$], N-channel ($n = 4$), and combined N- and P-channel block ($n = 4$) on the modulation by oxo-M.

ChAT mRNA, on the other hand, is a less equivocal criterion. Its sufficiency seems justified in light of the strong correlation between the presence of ChAT mRNA and protein (Butcher et al., 1993) and the limitation of these markers to the neostriatal interneuronal population (Bolam and Bennett, 1995).

The expression pattern of muscarinic receptor mRNAs in these neurons was also consistent with their identification as cholinergic interneurons. As found in previous *in situ* hybridization (Weiner et al., 1990) and immunocytochemical studies (Levey et al., 1991) of large aspiny neostriatal neurons, the most abundant muscarinic receptors in cholinergic interneurons seemed to be of the m2-subtype. Our multiplex PCR results suggest that m4 mRNA was also expressed by most cholinergic interneurons but in lower abundance, whereas m1 mRNA was expressed in only 20–30% of interneurons. This finding contrasts somewhat with that of Bernard et al. (1992) who found extensive colocalization of m1, m2, and m4 mRNAs in cholinergic interneurons. Our failure to observe colocalization was not caused by our inability to detect m1 mRNA per se, because it is seen in nearly all medium-sized spiny projection neurons using identical techniques ($n > 50$) (our unpublished observations). Another possible explanation for the difference is that m1 receptor mRNA was present but below our level of detection. This seems unlikely, however, for two reasons. First, PCR-based approaches like the ones used here have a

significantly lower detection threshold than conventional *in situ* hybridization techniques (Chesselet et al., 1995). Second, the physiological assays of muscarinic receptor function were consistent with the presence of M2-class receptors (m2, m4) but not M1-class receptors (m1, m3, m5). If present, these receptors would have been restricted necessarily to regions lost during the dissociation, such as distal dendrites and axon terminals. Nevertheless, we cannot exclude definitively the possibility that m1 mRNA was present but not detected.

Activation of muscarinic receptors led to a reduction in currents carried by N- and P-type Ca^{2+} channels. In addition to being antagonized by atropine, the modulation produced by oxo-M was dose-dependent, with EC_{50} values very close to those found for the m2 receptor-mediated modulation of Ca^{2+} currents in cholinergic neurons of the basal forebrain (Allen and Brown, 1993). In neostriatal cholinergic interneurons, as in these basal forebrain and peripheral neurons expressing M2-class receptors, the muscarinic modulation was blocked by application of NEM (Shapiro et al., 1994) or incubation with PTX (Beech et al., 1992; Allen and Brown, 1993). Although both G_i- and G_o-class G-proteins are PTX-sensitive, G_o-class proteins seem to be the most likely candidates for inhibition of N- and presumably P-type currents (Hille, 1994).

G_o-class proteins have been shown in peripheral neurons to rapidly modulate N-type currents through a membrane-delimited pathway (Hille, 1994; Wanke et al., 1994). The kinetics of the modulation in neostriatal interneurons is consistent with mediation by a similar signaling pathway (Bernheim et al., 1991; Boland and Bean, 1993). More direct evidence for a membrane-delimited pathway comes from the failure of bath-applied agonists to reduce currents in cell-attached patch recordings. This interpretation assumes that targeted N- and P-type channels were present in the patch. Although this was not verified directly, N-type currents were very prominent components of whole-cell currents from the somatodendritic membrane. It seems highly unlikely that all of the studied macropatches (containing 20–50 channels) would lack a significant complement of N-type channels. The only other signaling pathway known to influence Ca^{2+} channels that couples to M2-class receptors in neurons is dependent on cAMP (Hulme et al., 1990); however, cAMP did not alter the ability of M2-class receptors to inhibit Ca^{2+} currents.

In many neurons, N-type Ca^{2+} channels are the principal targets of the membrane-delimited pathway (Hille, 1994). N-type currents and at least four other types of high-voltage activated (HVA) Ca^{2+} currents were expressed in cholinergic interneurons. In agreement with previous studies of these neurons (Wilson et al., 1990; Kawaguchi, 1993), low-voltage activated currents were not seen. The RT-PCR profiles of α1-subunit mRNA (showing class A, B, C/D, and E mRNA coexpression) were in good agreement with the pharmacological profiles showing colocalization of Q-, N-, L-, P-, and R-type currents. The molecular demonstration of class B mRNA expression increases the plausibility of the proposition that the molecular features of the signaling pathway in neostriatal interneurons are similar to those found in other cell types in which N-type (class B) channels are modulated. The M2-class receptor modulation was not limited to N-type channels, however. As in cholinergic neurons of the basal forebrain (Allen and Brown, 1993), a component of the dihydropyridine resistant (non-L-type) current was modulated after exposure to ω-CgTx GVIA. Our results suggest that a portion of this oxo-M-sensitive current is of the P-type. P-type Ca^{2+} currents are reduced by G-protein pathways in a number of other brain neurons (Mintz and Bean, 1993; Howe and Surmeier, 1995; Foehring, in press).

Functional consequences

Because of the well established role of N- and P-type Ca^{2+} channels in the regulation of neurotransmitter release (Dunlap et al., 1995), our results provide a mechanism for homo- or heterosynaptic inhibition of ACh release in the striatum (James and Cubeddu, 1987; Lapchak et al., 1989; Dolezal and Wecker, 1990). The reliance on a membrane-delimited signaling pathway would endow this modulation with not only rapid kinetics but also a spatially restricted focus (Brown, 1993).

Muscarinic reduction of dendritic Ca^{2+} currents through N- and P-type channels should also attenuate dendritic invasion of initial segment spikes (Spruston et al., 1995) and the active augmentation of excitatory synaptic events arising from cortical or thalamic sources (Wilson, 1993; Bernander et al., 1994). Because membrane-delimited signaling is spatially and temporally focused, this type of control could be of importance in regulating the computational functions of dendrites. The voltage-dependence of the modulation raises the intriguing possibility that postsynaptic regenerative events could be used as feedback signal, momentarily reversing muscarinic changes in dendritic computations (Spruston et al., 1995).

REFERENCES

Akins PT, Surmeier DJ, Kitai ST (1990) Muscarinic modulation of a transient K^+ conductance in rat neostriatal neurons. Nature 344: 240–242.

Allen TG, Brown DA (1993) M2 muscarinic receptor-mediated inhibition of the Ca^{2+} current in rat magnocellular cholinergic basal forebrain neurones. J Physiol (Lond) 466:173–189.

Barbeau A (1962) The pathogenesis of Parkinson's disease: a new hypothesis. Can Med Assoc J 87:802–807.

Bargas J, Howe A, Eberwine J, Cao Y, Surmeier DJ (1994) Cellular and molecular characterization of Ca^{2+} currents in acutely-isolated, adult rat neostriatal neurons. J Neurosci 14:6667–6686.

Bargas J, Surmeier DJ, Kitai ST (1991) High- and low-voltage activated calcium currents are expressed by rat neostriatal neurons. Brain Res 541:70–74.

Bean BP (1989) Neurotransmitter inhibition of neuronal calcium currents by changes in channel voltage dependence. Nature 340:153–156.

Beech DJ, Bernheim L, Hille B (1992) Pertussis toxin and voltage dependence distinguish multiple pathways modulating calcium channels of rat sympathetic neurons. Neuron 8:97–106.

Bernander O, Koch C, Douglas RJ (1994) Amplification and linearization of distal synaptic input to cortical pyramidal cells. J Neurophysiol 72:2743–2753.

Bernard V, Normand E, Bloch B (1992) Phenotypical characterization of the rat striatal neurons expressing muscarinic receptor genes. J Neurosci 12:3591–3600.

Bernheim L, Beech DJ, Hille B (1991) A diffusible second messenger mediates one of the pathways coupling receptors to calcium channels in rat sympathetic neurons. Neuron 6:859–867.

Bernheim L, Mathie A, Hille B (1992) Characterization of muscarinic receptor subtypes inhibiting Ca^{2+} current and M current in rat sympathetic neurons. Proc Natl Acad Sci USA 89:9544–9548.

Bolam JP, Bennett BD (1995) Microcircuitry of the neostriatum. In: Molecular and cellular mechanisms of the neostriatum (Ariano MA, Surmeier DJ, eds), pp 1–20. Austin, TX: R. G. Landes.

Boland LM, Bean BP (1993) Modulation of N-type calcium channels in bullfrog sympathetic neurons by luteinizing hormone-releasing hormone: kinetics and voltage dependence. J Neurosci 13:516–533.

Bonner TI (1992) Domains of muscarinic acetylcholine receptors that confer specificity of G protein coupling. Trends Pharmacol Sci 13:48–50.

Bonner TI, Buckley NJ, Young AC, Brann MR (1987) Identification of a family of muscarinic acetylcholine receptor genes. Science 237:527–532.

Bonner TI, Young AC, Brann MR, Buckley NJ (1988) Cloning and expression of the human and rat m5 muscarinic acetylcholine receptor genes. Neuron 1:403–410.

Brice A, Berrard S, Raynaud B, Ansieau S, Coppola T, Weber MJ, Mallet J (1989) Complete sequence of a cDNA encoding an active rat choline acetyltransferase: a tool to investigate the plasticity of cholinergic phenotype expression. J Neurosci Res 23:266–273.

Brown AM (1993) Membrane-delimited cell signaling complexes: direct ion channel regulation by G proteins. J Membr Biol 131:93–104.

Butcher LL, Oh JD, Woolf NJ (1993) Cholinergic neurons identified by in situ hybridization histochemistry. Prog Brain Res 98:1–8.

Cheney DL, Lefevre HF, Racagni G (1975) Choline acetyltransferase activity and mass fragmentographic measurement of acetylcholine in specific nuclei and tracts of rat brain. Neuropharmacology 14: 801–809.

Chesselet M, Delfs JM, Gasemzadeh B, Lenz S, Mercugliano M, Qin Y, Salin P, Soghomonian J (1995) Cell specific mRNA expression in the striatum. In: Molecular and cellular mechanisms of the neostriatum (Ariano MA, Surmeier DJ, eds), pp 89–102. Austin, TX: R. G. Landes.

Dolezal V, Wecker L (1990) Muscarinic receptor blockade increases basal acetylcholine release from striatal slices. J Pharmacol Exp Ther 252:739–743.

Dubel SJ, Starr TV, Hell J, Ahlijanian MK, Enyeart JJ, Catterall WA, Snutch TP (1992) Molecular cloning of the alpha-1 subunit of an omega-conotoxin-sensitive calcium channel. Proc Natl Acad Sci USA 89:5058–5062.

Dunlap K, Luebke JI, Turner TJ (1995) Exocytotic Ca^{2+} channels in mammalian central neurons. Trends Neurosci 18:89–98.

Foehring RC (1996) Serotonin modulates N- and P-type calcium currents in neocortical pyramidal neurons via a membrane delimited pathway. J Neurophysiol, in press.

Graybiel AM (1990) Neurotransmitters and neuromodulators in the basal ganglia. Trends Neurosci 13:244–254.

Hamill OP, Marty A, Neher E, Sakmann B, Sigworth FJ (1981) Improved patch-clamp techniques for high resolution current recording from cells and cell-free membrane patches. Pflügers Arch 391:85–100.

Hersch SM, Gutekunst CA, Rees HD, Heilman CJ, Levey AI (1994) Distribution of m1–m4 muscarinic receptor proteins in the rat striatum: light and electron microscopic immunocytochemistry using subtype-specific antibodies. J Neurosci 14:3351–3363.

Hescheler H, Kameyama M, Trautwein W (1986) On the mechanism of muscarinic inhibition of the cardiac Ca current. Pflügers Arch 407:182–189.

Hille B (1994) Modulation of ion-channel function by G-protein-coupled receptors. Trends Neurosci 17:531–536.

Howe AR, Surmeier DJ (1995) Muscarinic receptors modulate N-, P- and L-type Ca^{2+} currents in rat striatal neurons through parallel pathways. J Neurosci 15:458–469.

Hui A, Ellinor PT, Krizanova O, Wang JJ, Diebold RJ, Schwartz A (1991) Molecular cloning of multiple subtypes of a novel rat brain isoform of the alpha 1 subunit of the voltage-dependent calcium channel. Neuron 7:35–44.

Hulme EC, Birdsall NJ, Buckley NJ (1990) Muscarinic receptor subtypes. Annu Rev Pharmacol Toxicol 30:633–673.

James MK, Cubeddu LX (1987) Pharmacologic characterization and functional role of muscarinic autoreceptors in the rabbit striatum. J Pharmacol Exp Ther 240:203–215.

Kawaguchi Y (1993) Physiological, morphological and histochemical characterization of three classes of interneurons in rat neostriatum. J Neurosci 13:4908–4923.

Lambolez B, Audinat E, Bochet P, Crepel F, Rossier J (1992) AMPA receptor subunits expressed by single Purkinje cells. Neuron 9:247–258.

Lapchak PA, Araujo DM, Quirion R, Collier B (1989) Binding sites for [^{3}H]AF-DX 116 and effect of AF-DX 116 on endogenous acetylcholine release from rat brain slices. Brain Res 496:285–294.

Levey AI, Kitt CA, Simonds WF, Price DL, Brann MR (1991) Identification and localization of muscarinic acetylcholine receptor proteins in brain with subtype-specific antibodies. J Neurosci 11:3218–3226.

Mathie A, Bernheim L, Hille B (1992) Inhibition of N- and L-type calcium channels by muscarinic receptor activation in rat sympathetic neurons. Neuron 8:907–914.

McGeer PL, McGeer EG, Singh VK, Chase WH (1974) Choline acetyltransferase localization in the central nervous system by immunohistochemistry. Brain Res 81:373–379.

Mintz IM, Bean BP (1993) GABAB receptor inhibition of P-type Ca^{2+} channels in central neurons. Neuron 10:889–898.

Misgeld U, Calabresi P, Dodt HU (1986) Muscarinic modulation of calcium dependent plateau potentials in rat neostriatal neurons. Pflügers Arch 407:482–487.

Misgeld U, Weiler MH, Bak IJ (1980) Intrinsic cholinergic excitation in the rat neostriatum: nicotinic and muscarinic receptors. Exp Brain Res 39:401–409.

Monyer H, Lambolez B (1995) Molecular biology and physiology at the single-cell level. Curr Opin Neurobiol 5:382–387.

Phelps PE, Houser CR, Vaughn JE (1985) Immunocytochemical localization of choline acetyltransferase within the rat neostriatum: a correlated light and electron microscopic study of cholinergic neurons and synapses. J Comp Neurol 238:286–307.

Randall A, Tsien RW (1995) Pharmacological dissection of multiple types of Ca^{2+} channel currents in rat cerebellar granule neurons. J Neurosci 15:2995–3012.

Shapiro MS, Wollmuth LP, Hille B (1994) Modulation of Ca^{2+} channels by PTX-sensitive G-proteins is blocked by *N*-ethylmaleimide in rat sympathetic neurons. J Neurosci 14:7109–7116.

Snutch TP, Reiner PB (1992) Ca^{2+} channels: diversity of form and function. Curr Opin Neurobiol 2:247–253.

Snutch TP, Tomlinson WJ, Leonard JP, Gilbert MM (1991) Distinct calcium channels are generated by alternative splicing and are differentially expressed in the mammalian CNS. Neuron 7:45–57.

Soong TW, Bourinet E, Slaymaker S, Mathews E, Dubel SJ, Vincent SR, Snutch TP (1994) Alternative splicing generates rat brain α1A calcium channel isoforms with distinct electrophysiological properties. Soc Neurosci Abstr 20:70.

Spruston N, Schiller Y, Stuart G, Sakmann B (1995) Activity-dependent action potential invasion and calcium influx into hippocampal CA1 dendrites. Science 268:297–300.

Starr TV, Prystay W, Snutch TP (1991) Primary structure of a calcium channel that is highly expressed in the rat cerebellum. Proc Natl Acad Sci USA 88:5621–5625.

Stea A, Tomlinson WJ, Soong TW, Bourinet E, Dubel SJ, Vincent SR, Snutch TP (1994) Localization and functional properties of a rat brain α1A calcium channel reflect similarities to neuronal Q- and P-type channels. Proc Natl Acad Sci USA 91:10576–10580.

Surmeier DJ, Bargas J, Hemmings Jr HC, Nairn AC, Greengard P (1995) Modulation of calcium currents by a D1 dopaminergic protein kinase/phosphatase cascade in rat neostriatal neurons. Neuron 14:385–397.

Surmeier DJ, Kita H, Kitai ST (1988) The expression of GABA and Leu-enkephalin immunoreactivity in primary cultures of rat neostriatum. Dev Brain Res 42:265–282.

Tsien RW, Ellinor PT, Horne WA (1991) Molecular diversity of voltage-dependent Ca^{2+} channels. Trends Pharmacol Sci 12:349–354.

Tsien RW, Lipscombe D, Madison DV, Bley KR, Fox AP (1995) Reflections on Ca(2+)-channel diversity, 1988–1994. Trends Neurosci 18:52–54.

Tukey JW (1977) Exploratory data analysis. Menlo Park, CA: Addison-Wesley.

Vilaró MT, Wiederhold KH, Palacios JM, Mengod G (1992) Muscarinic M2 receptor mRNA expression and receptor binding in cholinergic and non-cholinergic cells in the rat brain: a correlative study using in situ hybridization histochemistry and receptor autoradiography. Neuroscience 47:367–393.

Wanke E, Bianchi L, Mantegazza M, Guattco E, Mancinelli E, Ferroni A (1994) Muscarinic regulation of Ca^{2+} currents in rat sensory neurons: channel and receptor types, dose–response relationships and cross-talk pathways. Eur J Neurosci 6:381–391.

Weiner DM, Levey AI, Brann MR (1990) Expression of muscarinic acetylcholine and dopamine receptor mRNAs in rat basal ganglia. Proc Natl Acad Sci USA 87:7050–7054.

Wilson CJ (1993) The generation of natural firing patterns in neostriatal neurons. In: Chemical signaling in the basal ganglia (Arbuthnott GW, Emson PC, eds), pp 277–297. Amsterdam: Elsevier.

Wilson CJ, Chang HT, Kitai ST (1990) Firing patterns and synaptic potentials of identified giant aspiny interneurons in the rat neostriatum. J Neurosci 10:508–519.

Wooten GF (1990) Parkinsonism. In: Neurobiology of disease (Pearlman AL, Collins RC, eds), pp 454–468. New York: Oxford UP.